Polymers

CrossMark

Preparation and characterization of highly conductive polyurethane composites containing graphene and gold nanoparticles

Nuha Y. Al-Attabi[1,2], Gagan Kaur[1], Raju Adhikari[1], Peter Cass[1], Mark Bown[1], Meg Evans[3], Pathiraja Gunatillake[1,*], François Malherbe[2], and Aimin Yu[2,*] (ID)

[1] CSIRO Manufacturing, Bayview Avenue, Clayton, VIC 3168, Australia

[2] Faculty of Science Engineering and Technology, Swinburne University of Technology, Hawthorn 3122, Australia

[3] CSIRO Manufacturing, Julius Avenue, North Ryde, NSW 2113, Australia

ABSTRACT

Two series of gold nanoparticles/graphene/polyurethane composite films were prepared using a solution mixing method. The first series was of constant loading of graphene/polyurethane with varying levels of gold nanoparticles (AuNPs), while the second was of varying graphene content with constant loading of AuNPs. The electrical conductivity of the AuNPs/graphene/polyurethane composites was determined using the two-point probe method. For the first series, a maximum conductivity of 0.424 S cm^{-1} was achieved with a 5% AuNPs/5% graphene/polyurethane composite, and for the second, a maximum conductivity of 1.388 S cm^{-1} was achieved with a 5% AuNPs/15% graphene/polyurethane composite. The composites were characterized by Fourier transform infrared spectroscopy, scanning electron microscopy, differential scanning calorimetry, thermogravimetric analysis, and tensile testing methods. Tensile strengths and thermogravimetric analyses showed, respectively, acceptable mechanical properties and thermal stability of the parent polyurethanes. Furthermore, cytotoxicity assay tests evidenced that AuNPs/graphene/polyurethane composites were not cytotoxic to living cells in vitro and, consequently, potentially useful in biomedical applications.

Introduction

Recently, electroconductive and electroactive polymers have attracted considerable interest due to their potential application in biosensors, drug delivery systems, biomedical implants and tissue engineering [1]. Common conducting polymers including polypyrrole, polyaniline and poly(3,4-ethylenedioxythiophene) (PEDOT) [2] have been shown to possess good electrical and optical properties, but their mechanical properties, biocompatibility and processability are often poor. Although

---

Address correspondence to E-mail: thilak.gunatillake@csiro.au; aiminyu@swin.edu.au

conventional conducting polymers are inherently non-biodegradable, some attempts have also been made to impart biodegradability by incorporating degradable linkages such as esters [3], although these attempts resulted in substandard materials. The development of polymer composites with conducting nanoparticles has been one of the interesting approaches to envisage overcoming some of these limitations [4]. Furthermore, increased attention has been directed towards electroconductive polymer composites comprised of biocompatible polymers, such as polyurethane, with dispersed conductive fillers. These include metallic nanoparticles such as silver (Ag), gold (Au), nickel (Ni) and copper (Cu), as well as carbon-based materials such as graphene [4]. Conducting polymers like polypyrrole and polyaniline have also been used as conducting fillers to compensate for their poor processability [5].

In general, polyurethanes (PUs) have good compatibility with tissues and blood, and they exhibit a relatively high mechanical strength. Various types of PUs have been evaluated for their stability in a biological environment using both in vitro and in vivo procedures [6]. Accordingly, PUs have successfully found applications in medical implants such as cardiac pacemakers, catheters, implantable prostheses, cardiac assist devices, heart valves and vascular grafts [7]. To date, most research on improving the conductivity of PU has focussed on incorporating conductive species into the polymers. It has been demonstrated that the resulting composites retain their biocompatibility, processability and biostability, but the mechanical properties were compromised [8, 9].

Gold nanoparticles (AuNPs) have received particular attention for in vivo applications owing to their proven high stability and biocompatibility [10, 11]. They also exhibit fascinating features such as size-dependent electronic, magnetic and optical properties. This has led to applications in catalysis and biology [12] due to their unique chemical and physical properties, and as such AuNPs have been used widely in the fabrication of biosensors for medical analysis.

In recent years, graphene and graphene-related materials have also been explored as conducting sheets. Graphene is a single-layer two-dimensional sp^2-hybridized carbon arranged in honeycomb lattice [13] which gives it electrical conductivity. Graphene sheets exhibit high electrical conductivity and thermal and mechanical properties [14]. Nanocomposites of graphene and metallic nanoparticles have promising applications in energy storage, chemical sensors and catalysis [15–17].

There have been several reports on the preparation of PU composites by adding either graphene or AuNPs into the network of PU. For example, Kaur et al. [4, 18] reported the fabrication of graphene/PU composites and the electrical conductivity, mechanical properties and cell viability of the materials. Hsu and Lin examined the surface morphological transformation and the cellular response of PU/AuNPs composite [19]. However, they did not investigate the electrical conductivity and mechanical properties of these materials. Shan et al. [20] constructed a novel enzyme immobilization matrix to combine the benefits of AuNPs, graphene and chitosan nanocomposites for biosensing applications. These composites showed high electrocatalytic activity, high sensitivity and good stability. However, the use of both gold nanoparticles and graphene in polyurethane composites has not been reported previously. The AuNPs and graphene in combination can be expected to form conducting pathways to improve conductivity, potentially forming composites with good mechanical properties useful in fabricating components for medical implants.

In this study, we report the preparation of PU/AuNPs/graphene composites and evaluate the effects of graphene and AuNPs on the electrical conductivity and mechanical properties of the resulting composites. Elast-Eon™, which is a biostable PU currently used in cardiac pacemaker lead insulations [21], is chosen as a base polymer for the preparation of novel composites. A series of PU composites with varying percentages of AuNPs and graphene are prepared and their electrical conductivities determined. The mechanical and thermal properties of AuNPs/graphene/PU composites are then investigated using a combination of tensile testing, differential scanning calorimetry (DSC) and thermogravimetric analysis (TGA). The composites are also characterized using scanning electron microscopy (SEM), Fourier transform infrared (FTIR) spectroscopy, energy-dispersive X-ray spectroscopy (EDX) and transmission electron microscopy (TEM), and their cytotoxicity is evaluated using an indirect cytotoxicity assay.

Materials and methods

Materials

Reagents including gold (III) chloride trihydrate (≥99.99%), trisodium citrate, oleylamine (technical grade, 70%) and tetrahydrofuran (THF) were purchased from Sigma-Aldrich. The thermoplastic polyurethane Elast-Eon^{TM} (E2A) was graciously offered by St Jude Medical (St Paul, Minnesota- USA) and was dried under vacuum (10 mbar) at 60 °C for 24 h before use. Graphene was purchased from JCNANO INC Advanced Materials Supplier (China, http://www.jcno.net/) and was used as received. Based on the manufacturer's supplied information, the graphene supplied was 2-nm-thick sheets with a purity of 98%. The conductivity was 10^5 S/m.

Synthesis of gold NPs

AuNPs were prepared using the Burst method [22]. Briefly, 45 mg of HAuCl$_4$ was dissolved in 150 μL of 37% HCl, followed by the addition of 0.75 mL oleylamine (0.114 mmol). The solution was kept at 60 °C on a hot plate with stirring for 10 min to homogenize and evaporate water. The temperature was increased to 120 °C, stirred for 20 min, then raised to 210 °C and stirred for another hour. The colour of the reacting mixture changed from yellow to red. After slowly cooling down to ambient temperature, the sample was washed twice with ethanol, followed by THF to remove the excess oleylamine. AuNPs were redispersed in THF and characterized by UV–Vis spectrometer (TECAN) and dynamic light scattering (DLS) using a Zeta Sizer Nano-ZS (Malvern).

Preparation of PU-based composites films

Two series of AuNPs/graphene/PU composite were prepared to determine the effect of AuNPs and graphene on conductivity: (1) varying AuNPs compositions with 5 wt% graphene concentration and (2) varying graphene concentration but with 5 wt% AuNPs. AuNPs/graphene/PU composites were prepared using a solution mixing method. Three hundred milligrams of PU and appropriate amounts of AuNPs and graphene were dissolved in 20 mL THF. The mixture was stirred overnight at 50 °C to homogenize the dispersion. The solution was then poured into a petri dish and dried in a vacuum oven

at 70 °C overnight. The sample was then removed from the oven, cut, weighed and pressed into a film by compression moulding at 200 °C under 6 tonnes pressure for 5 min.

Measurement of conductivity

The composites were compression-moulded into films around 100 μm thick, and strips of 1 × 2.5 cm were cut from films. The strip sample was pasted on a glass microscope slide and then electrical contacts formed using conductive silver paint along the long sides. DC resistance measurements of these composites films were measured by two-point probe configuration using a Keithley 2400 Source Meter unit by current, and the measuring voltage range is $1.6 × 10^{-2}$–8.5 V. The electrical conductivity was calculated using the equation below:

The resistivity ρ, in Ω cm, was calculated, using the equation:

$$\rho = \frac{R \times L \times d}{a}$$

$$\rho = \frac{V \times L \times d}{I \times a}, \text{ in } \Omega \text{ cm},$$

where R = electrical resistance (Ω), V = voltage (V), I = current (A), L = electrode length (cm), d = film thickness (cm), and a = electrode separation (cm).

The conductivity δ was then calculated by using the equation below:

$$\delta = 1/\rho, \text{ in S cm}^{-1}.$$

The conductivity values were reported as the average of three replicates.

Characterization

The Fourier transform infrared (FTIR) spectroscopy analysis spectra of the composites films and control were recorded by an FTIR spectrometer (Thermo Scientific, Nicolet iS5, USA) and OMNIC in the middle infrared range 600–4000 cm^{-1}. The morphology and EDX analysis of films were operated using a ZEISS MERLIN Ultra High Resolution field emission scanning electron microscope (FE-SEM) at an accelerating voltage of 7–20 kV. For cross-sectional SEM analysis, the composites films were etched using a 20 wt% potassium hydroxide ethanol solution for one minute followed by washing with deionized water, and air-dried. All film samples were coated with

~20-nm-thick iridium prior to analysis. JEOL JEM3010 field high-resolution emission transmission electron microscopy (TEM) was used to obtain the TEM images. The thermal properties of the composite films were examined using a Mettler Toledo DSC 821 differential scanning calorimetry (DSC). Samples were heated from −50 to 250 °C at a rate of 5 °C/min under a nitrogen purge of 30 mL/min. Each sample was run in triplicate, and the results were processed using STARe software. A Mettler Toledo TGA/SDTA 851 thermogravimetric analyser and STARe software were used to measure the changes in weight of the composite materials as a function of temperature. The analysis of all the composites films was carried out under nitrogen atmosphere. Tensile strength (TS) testing was carried out on pressed composites samples 0.3–0.5 μm thick using ASTM D882 method in a Instron 5565 Testing Machine. The materials were cut into dumbbell-shaped samples of 3 × 1 cm and were conditioned. A 1-kN load cell was utilized, and the crosshead speed was 10 mm/min. Reported results are the mean values of four replicates.

Assessment of the in vitro cytotoxicity

An indirect cytotoxicity test was used to test the AuNP/graphene/PU composite films. The samples were placed into a humidified box and put onto a gently rocking platform for 66 h. The supernatant liquid was collected into a sterile tube and stored at 4 °C until tested. The extracts from each sample were prepared in a double-diluting series in serum-free culture medium [SFM = cell culture medium MEM with additives, non-essential amino acids (NEAA), and insulin/selenium/transferring (IST)] and tested against L929 mouse fibroblast cells that had been pre-seeded in a 96-well TCPS plate 24 h before. Cells viability was evaluated 24 h after the addition of extract dilutions to cells using an MTT (3-(4,5-dimethylthiazol-2-yl)-2,5-diphenyltetrazolium bromide) assay that measures metabolic activity. Each 96-well TCPS test plate also included three internal controls, as follows:

1. Serum-free medium (SFM) to calibrate the assay to 100%
2. SFM + 5% phosphate-buffered saline (PBS) and
3. SFM + 5% dimethylsulphoxide (DMSO).

Representative phase contrast images of representative wells of each of the extracts and control solution dilutions were taken after 20 h of culture, prior to the addition of MTT reagent.

Results and discussion

Morphology and structure of composites

Monodispersed AuNPs were prepared using the Burst method [22], where gold (III) chloride trihydrate (HAuCl$_4$) was mixed with oleylamine, a capping and stabilizing agent. The formation of AuNPs was evidenced by the colour change of the solution from yellow to wine red and the distinct surface plasmon resonance peak at 523 nm. As measured by DLS, the average size of the particles was 18.2 nm with a polydispersity of 0.098. These results confirmed that AuNPs with narrow polydispersity were successfully produced, and the results are in agreement with literature values [22].

AuNPs/graphene/PU composites were then prepared using the solution (THF as solvent) mixing method. The morphology of the prepared composites and their internal structure were firstly characterized by the cross-sectional SEM. Figure 1 shows representative SEM images of virgin PU and composite films with varying compositions of AuNPs and graphene. As expected, the PU film without any filler (Fig. 1a) exhibited a smooth surface, indicating a uniform distribution of the polymer network. Figure 1b shows a relatively uniform distribution of graphene in PU. However, the cross-sectional structure of AuNPs-loaded PU film represented a fairly uniform distribution of spheric particles with a few aggregates (Fig. 1c). The surface topography of PU films with both AuNPs and graphene (Fig. 1d–f) was relatively different, exhibiting a random surface pattern. However, as seen from Fig. 1e, f, the distribution of AuNPs and graphene was relatively uniform.

Further evidence for particle distribution was observed in EDX spectra. The presence of AuNPs could be seen in the images generated by the EDX analysis shown in Fig. 2. The EDX profile showed a strong signal for gold nanoparticles which were uniformly distributed in the whole polymer matrix.

The distribution of AuNPs and graphene within the composite films was further characterized by TEM. Figure 3 shows representative TEM micrographs of PU and composites varying in compositions of AuNPs and graphene. Figure 3a shows Elast-
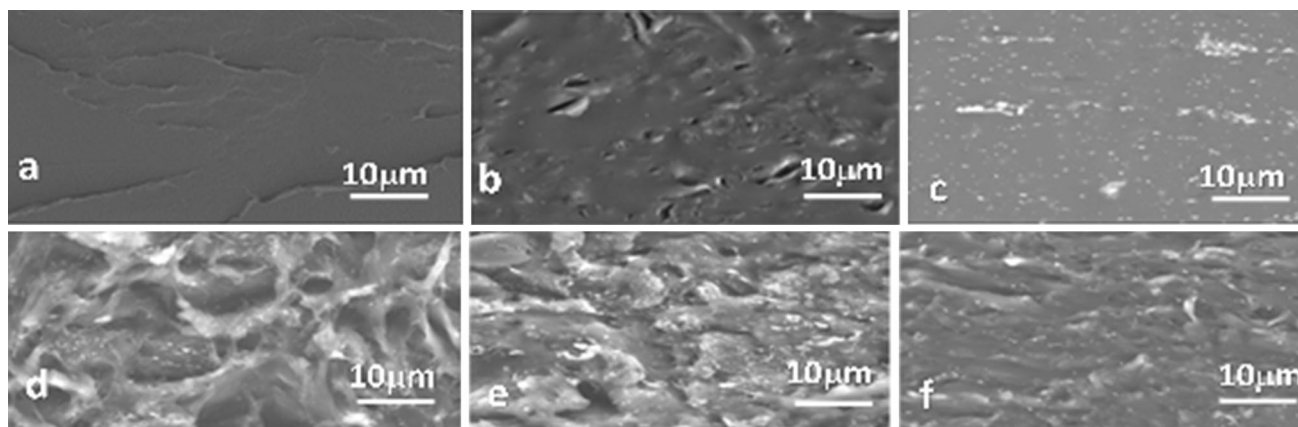
Figure 1 Cross-sectional SEM images of PU **a** PU, **b** 5% graphene/PU, **c** 5% AuNPs/PU, **d** 5% AuNPs/5% graphene/PU, **e** 20% AuNPs/ 5% graphene/PU and **f** 15% graphene/5% AuNPs/PU composite films.
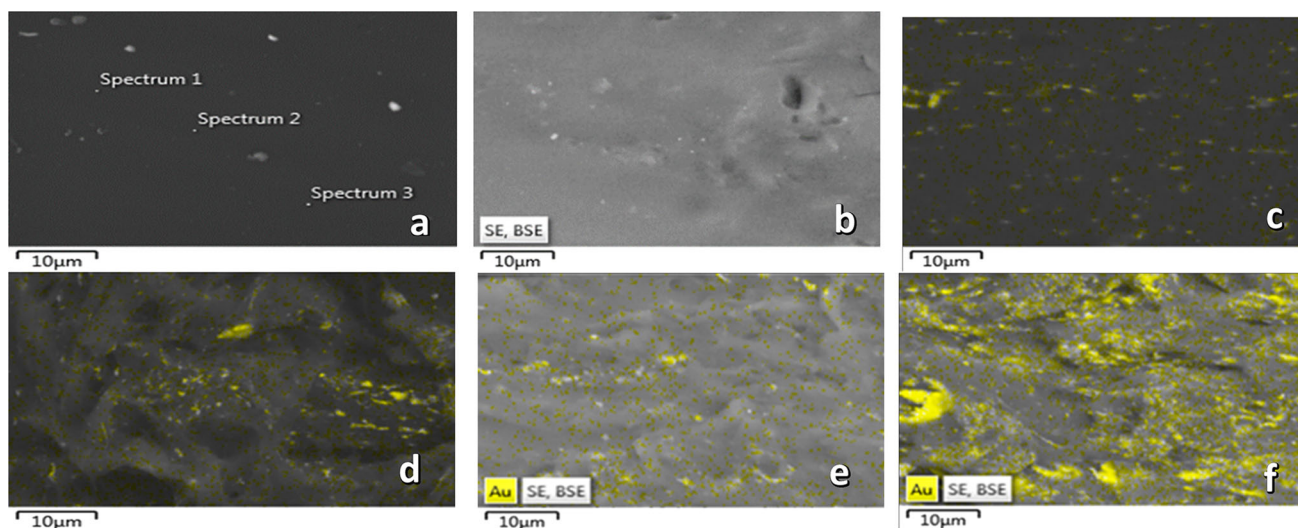

Figure 2 EDX spectroscopy of **a** Elast-Eon^{TM} PU (spectra 1, 2 and 3 refer to the points scanned to generate elemental composition data), **b** 5% Graphene/PU, **c** 5% AuNPs/PU, **d** 5% AuNPs/ 5% Graphene/PU, **e** 15% graphene/5% AuNPs/PU and **f** 20% AuNPs/5% graphene/PU composite films.

Eon PU with no fillers where the sample appears to be more homogeneous. The image of graphene/PU composite (Fig. 3b) illustrates the sheet-like appearance of graphene covered by PU [20]. Figure 3c gives clear evidence of the spherical nature of AuNPs, and Fig. 3d shows graphene sheets around AuNPs/PU composites [23]. When increasing the concentration of AuNPs to 20%, aggregation of NPs is clearly observed (Fig. 3e). This observation supports the previous finding that increasing AuNPs concentration did not increase the conductivity in Series 1.

The FTIR analyses of PU-based films modified with varying loading of AuNPs and graphene were carried out to investigate whether fillers contributed to

the change in two-phase morphology of polyurethanes.

The FTIR spectra of PUs before and after blending with AuNPs and graphene did not show any significant changes. All Elast-Eon^{TM} PU composites films show distinct peaks at approximately 800 cm^{-1} for Si–C in Si-CH$_3$ [21], two intense peaks at 1016 and 1081 cm^{-1}, associated with Si–O–Si-stretching bands within PDMS segments [7, 24, 25], 1227 cm^{-1} peak for C-N stretch, 1260 cm^{-1} peak for C-H in Si-CH$_3$, 1535 cm^{-1} for N–H bend and C–N stretch, 1600 cm^{-1} for C=C stretch of benzene ring. Elast-Eon^{TM} PU also exhibited two peaks related to carbonyl groups: one at 1732 cm^{-1} associated with non-H-bonded
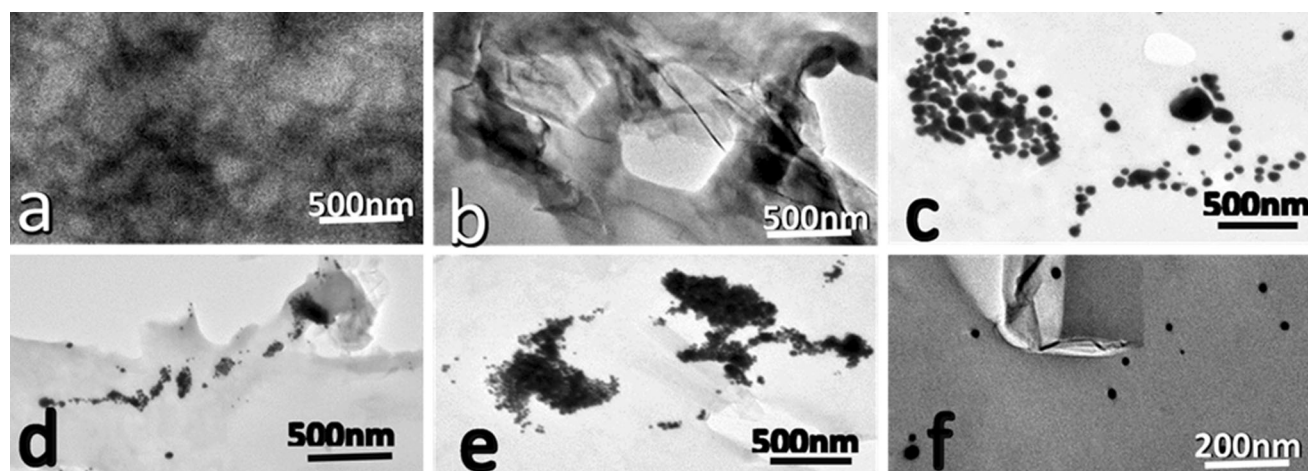
Figure 3 TEM images of **a** PU, **b** 5% graphene/PU, **c** 5% AuNPs/PU, **d** 5% AuNPs/5% graphene/PU, **e** 20% AuNPs/5% graphene/PU and **f** 5% AuNPs/15% graphene/PU composite films.

urethane carbonyls and the other at 1700 cm^{-1} corresponding to H-bonded urethane carbonyls [21]. All composites films had absorption band around the 1730 cm^{-1} except for the film made up of PU/5% AuNPs, which might be due to some degree of disruption of H-bonding in the presence of AuNPs. No significant changes in N–H absorption around 3500–3200 cm^{-1} were observed for composites in the series. It has been reported that N–H absorption bands in oleylamine may also appear in the same region [22, 26]. Overall, the FTIR spectra do not provide evidence that the incorporated AuNPs and graphene strongly interact with PU chains to cause a significant change in inter-chain hydrogen bonding to affect PU morphology, and exception may be for the sample shown in Fig. 4b.

Electrical conductivity of AuNPs/graphene/PU composite films

The PU (Elast-Eon^{TM}) material used in this study is typically non-conductive, with a measured conductivity of 1×10^{-14} S cm^{-1}, which is within the reported range of 10^{-11}–10^{-14} S cm^{-1} [27]. From the two series of AuNPs/graphene/PU prepared, it is noted that a 5% loading of graphene could dramatically increase the conductivity of PU to 2.5×10^{-2} S cm^{-1}. This is attributed to the high conductivity of graphene (10^3 S cm^{-1}) and its layered structure offering very high surface area [28].

Series 1 PU composites, with a constant 5% graphene and varied concentrations of AuNPs (0, 5, 15 and 20%), were prepared, and the measured

conductivity results are presented in Fig. 5 (curve a). The highest conductivity, 0.35 S cm^{-1}, was achieved for the composite with 5% graphene and 5% AuNPs. This value corresponds to an increase of over 13-fold compared to that of the material without gold. Further increase in AuNPs loading resulted in the decrease in conductivity, most probably due to self-aggregation of the NPs. It appears that the incorporation of AuNPs helped in creating new conductive pathways within the composite matrix by interaction with the graphene nanosheets [29].

Figure 5 curve b shows the electrical conductivity of composites with a fixed concentration of AuNPs and different loadings of graphene. It is noteworthy that the conductivity achieved with 5% loading of graphene (0.424 S cm^{-1}) was nearly tenfold higher than that achieved with only 5% loading of gold nanoparticles (3.6×10^{-10} S cm^{-1}). The excellent electrical conductivity of graphene and its layered structure together with the very high surface area may be the contributing factors to generate significantly higher conductive pathways compared to what can be achieved with spherical gold nanoparticles alone. The highest conductivity of 1.388 S cm^{-1} was achieved for the composite made of 5% gold nanoparticles and 15% grapheme, which represents a dramatic improvement when compared to 3.604×10^{-10} S cm^{-1} for conductivity of the parent composite with 5% AuNPs. This trend was not observed when the graphene loading was increased to 20% level; particle aggregation may be the contributing factor.
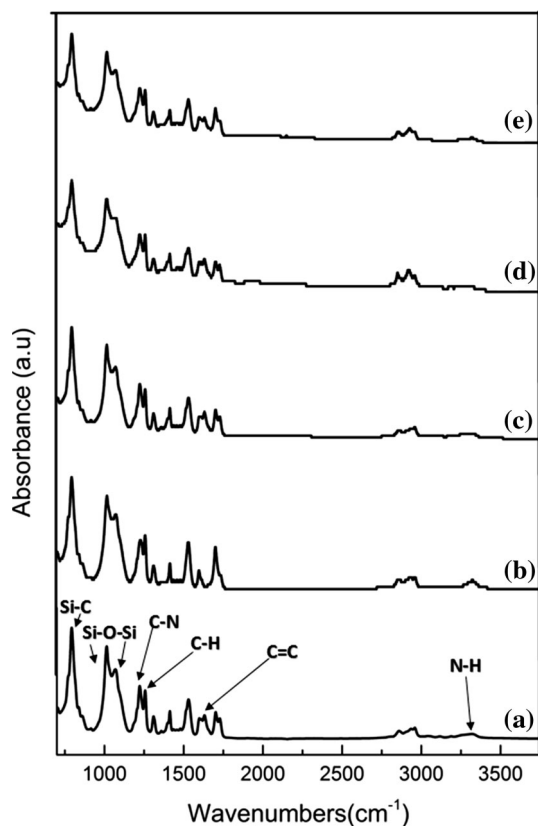
Figure 4 FTIR spectra of *a* Elast-Eon^{TM} PU *b* 5% AuNPs/PU *c* 5% graphene/PU *d* 5% AuNPs/5% graphene/PU *e* 5% AuNPs/15% graphene/PU composite films.

Thermal properties of composites

The thermal properties of AuNPs/graphene/PU composites were investigated by DSC and TGA in an attempt to understand the extent of interaction of these nanoparticles with the polyurethane matrix. Any molecular level interaction may influence the segmental motion of the PU, resulting in corresponding shifts of thermal stability and respective transition temperatures.

The DSC plots of PU, AuNPs/PU, graphene/PU and AuNPs/graphene/PU composites are shown in Fig. 6. The melting and glass transition temperatures reflect the extent of the soft and hard segmental phase interactions, and the resulting influence on PU morphology. The temperatures at which the melting of the crystalline domains of PU occurs help determine the optimum temperatures for processing [30]. Elast-Eon^{TM} is a polyurethane consisting of soft segment derived from a mixture of polydimethylsiloxane and poly(hexamethylene) macrodiols, and hard segment derived from 4,4'-methylenediphenyl diisocyanate
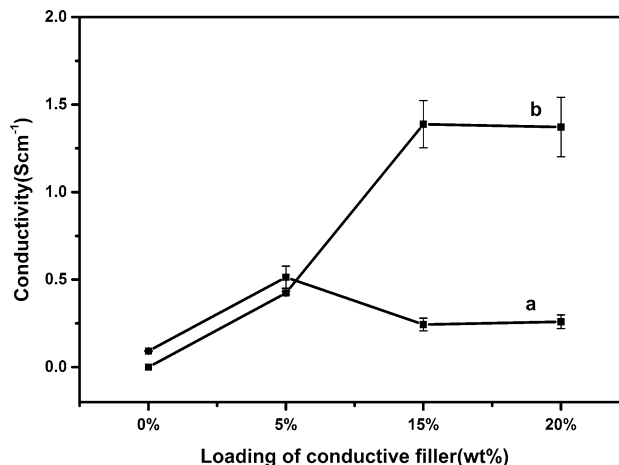

Figure 5 Electrical conductivity of *a* Series 1 PU composites containing 5% of graphene with varied loading of AuNPs and *b* Series 2 PU composites containing 5% of AuNPs with varied loading of graphene.

(MDI) and 1,4-butanediol (BDO) [7]. The DSC trace of Elast-Eon (Fig. 6a) exhibits a broad melting endotherm centred around 175 °C and sharp endotherm in the 220–230 °C, due to hard segment melting, and two other transitions due to either soft segment melting or glass transition [7]. The transition temperatures of the composite are significantly less resolved, hinting particles dispersion within the polyurethane matrix may have influenced the ordering of the soft and hard segments and more pronounced in the hard segment. In this series, all the polyurethane-based composites showed what appears to be a weak melting/glass transition around 65 °C, most likely resulting from single MDI units [7] formed by linking of soft segment MDI unit. All composite film showed a major endotherm around at lower temperature 150 °C compared to the Elast-Eon control at 170 °C, indicating some influence of the NPs on the ordering of the hard segments. When both AuNPs and graphene (Fig. 6b, c) were present at 5% level, a melting endotherm at a higher temperature (230 °C) indicative of some sort of ordering to form segregated microdomains was observed [31]. However, increasing the graphene loading to 15% (Fig. 6e) appears to have no significant effect of the PU. Further investigations using wide- and small-angle X-ray scattering techniques are needed to better understand the influence of AuNPs and graphene on PU morphology.

TGA was carried out to assess the impacts of incorporating NPs to PU. The results showed no such

significant effect on the thermal stability of the polyurethane. The onset of significant decomposition of the PU composite was around 250 °C, and this temperature was slightly higher for the composites. The rate of weight loss for composites was very similar for all samples up to about 350 °C. Overall, it can be mostly concluded that the effect of NPS on PU thermal stability is very minor.

Mechanical properties of composites

The mechanical properties of control (Elast-Eon™) and 5% AuNPs/5% Graphene/PU composite films are shown in Fig. 7 and Table 1. A can be seen, the addition of 5% AuNPs and 5% graphene to PU (Elast-Eon™) has a significant effect on both the elasticity
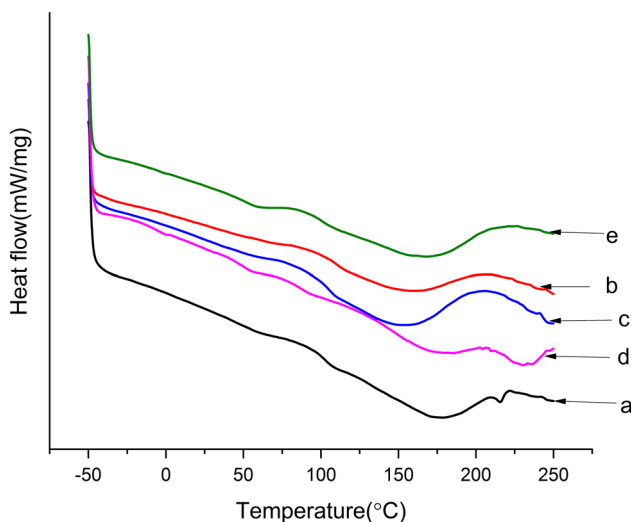
Figure 6 DSC plots of *a* PU, *b* 5% graphene/PU, *c* 5% AuNPs/PU, *d* 5% AuNPs/5% graphene/PU and *e* 5% AuNPs/15% graphene/PU composite films.
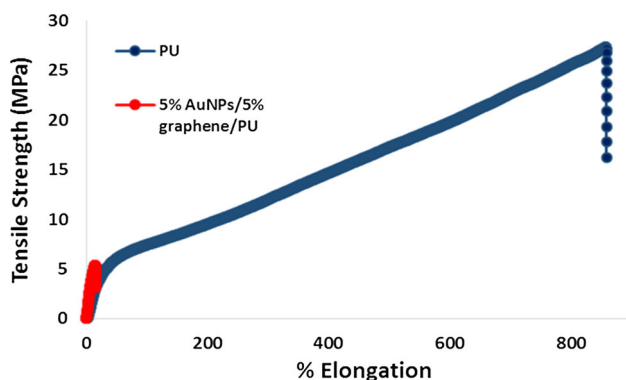
Figure 7 Tensile testing curves of PU (Elast-Eon™) and 5% AuNPs/5% graphene/PU composite film.

and the tensile strength of this composite. The AuNPs/graphene/PU composite exhibited a tensile strength of about 5.18 MPa, 80% less than that of the non-modified PU and a dramatic loss in elongation of the composite film down to ~13%, which is ~98% less than that of Elast-Eon™. The lower tensile strength and elongation are most likely due to the incorporation of AuNPs and graphene nanosheets, and some AuNPs form large agglomeration (micron-size-range particles) [18, 32, 33]. A similar observation was made for graphene/PU composites where tensile strength and elongation dropped with graphene loading [18].

It is also evident that the modification with AuNPs and graphene contributed to a significant increase in the modulus of PU composites. For example, following the addition of 5% AuNPs and 5% graphene, the modulus value of Elast-Eon™ increased from 8 to 26 MPa.

The poor mechanical properties compared to the pure PU may be a reflection of the NPs not being homogeneously dispersed within the polymer matrix which may lead to some degree of particle aggregation contributing to poor mechanical properties. The morphology characterization data also supported this as mentioned above.

## Cytotoxicity of AuNPs/graphene/PU composites

The in vitro cytotoxicity of AuNPs/graphene/PU composite film was tested using an indirect cytotoxicity MTT assay. Extracts from each sample were prepared in a double-diluting series in serum-free culture medium (SFM) and tested against L929 mouse fibroblast cells pre-seeded in a 96-well TCPS plate 24 h before. The starting dilution for each extract was described as 100% or neat, and this was diluted across nine wells of the plate in SFM such as 100% (neat), 50, 25, 12.5, 6.25, 3.125, 1.56, 0.78 and 0.39%. Cell viability was evaluated 24 h after the addition of extracts. A cell viability of less than 70% is deemed to be cytotoxic and at or above 70% is considered to be acceptable [34].

According to the outcomes of the MTT assay presented in Fig. 8a, cell viability levels were at an acceptable level at all dilutions of the extract of the PU control, and all points on PU graph were above the 70% level. The data confirm that there is no evidence of cytotoxicity associated with any

Table 1 Mechanical properties of 5% AuNPs/5% graphene/PU composite versus PU (Elast-Eon™)

	Elast-Eon™	AuNPs/graphene/PU	Change in property upon addition of AuNPs and graphene (%)
Tensile strength (MPa)	27 ± 1.2	5 ± 0.5	−81
Modulus of elasticity (MPa)	8 ± 0.8	26 ± 1.4	+225
Elongation at break (%)	>854 ± 0.8	>13.4 ± 0.3	−98

Figure 8 Cells viability after 24-h exposure to a diluting series of the extract (cell viability less than 70% is deemed to be cytotoxic which is marked on each graph with a *dashed red line*). Cell culture controls included cells seeded into uncoated wells in SFM, 5% PBS in SFM and 5% DMSO in SFM.
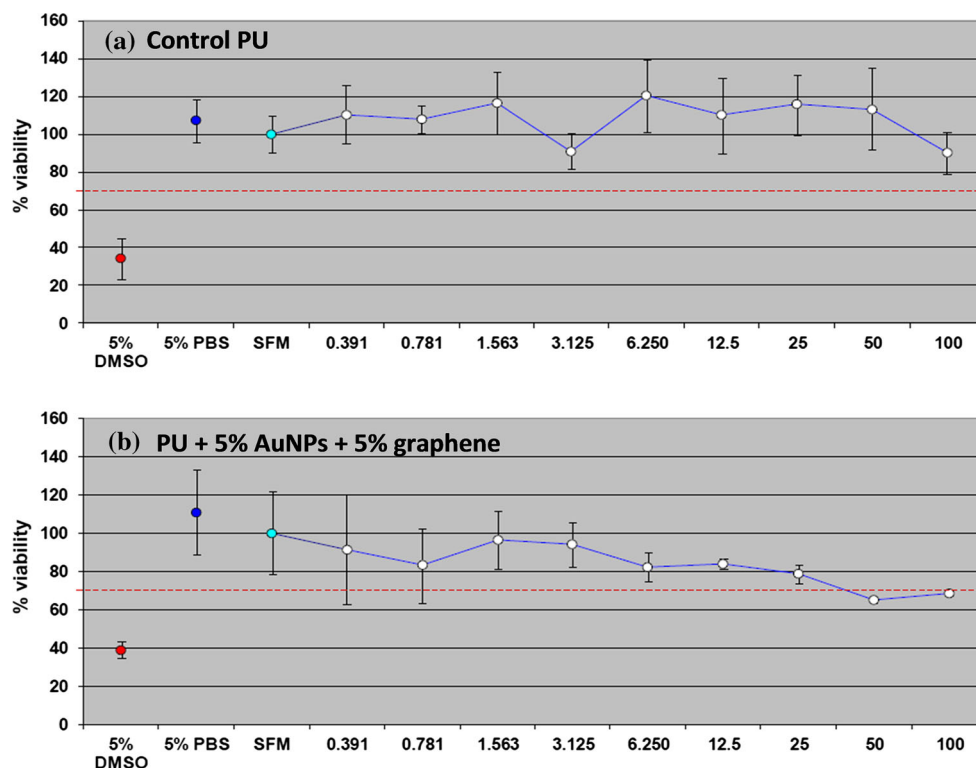
extractable when tested over period of 24 h. Figure 8b illustrates the results of the extract from the 5% AuNPs/5% graphene/PU composite. The cell viability levels were at an acceptable level with dilutions of 25% or below. With dilutions of 50 and 100%, the cell viability fell just below the acceptable level of 70% viability. The results indicate that there were subtle effects of higher concentrations of the extract of 5% AuNPs/5% graphene/PU on cell viability, but it was acceptable at or below 25% dilution.

Conclusions

Conductive PU (Elast-Eon™) composites of AuNPs and graphene were prepared using the solution mixing method, and the electrical conductivity of composite films was determined using the two-point probe method. The results showed that the addition of AuNPs significantly enhances the conductivity of graphene/PU composites. The conductivity of graphene/PU composite films with 5% loading of graphene was 2.5×10^{-2} S cm^{-1}, which increased to 0.42 S cm^{-1} with the addition of 5% AuNPs. Furthermore, the highest conductivity achieved was 1.388 S cm^{-1} for composites containing 5% loading of AuNPs and 15% of graphene. FTIR spectra showed that the incorporation of polyurethane with AuNPs and graphene did not show any significant changes to the polymer network. The mechanical properties of AuNPs/graphene/PU composites were poor, showing a significant loss of tensile strength and elongation compared to the unmodified polyurethane. This may be a reflection of the presence of a significant level of particle agglomerates creating defects within

the matrix leading to poor mechanical strength. Additionally, cell-based cytotoxicity tests showed that the PU control, PU + 5% graphene and PU + 5% AuNPs composite films have no evidence of release of cytotoxic compounds when cells were exposed to dilutions of extract during a 24-h period. However, there were subtle effects of higher concentrations of the extract of PU + 5% AuNPs + 5% graphene on both cell viability, but it was acceptable at or below 25% dilution. Overall the combination of AuNPs and graphene has enabled the fabrication of PU composites with high conductivity but with a major compromise in mechanical properties.

Acknowledgements

Compliance with ethical standards

Conflict of interest We wish to confirm that there are no known conflicts of interest associated with this publication and there has been no significant financial support for this work that could have influenced its outcome.

References

[1] Jagur-Grodzinski J (2012) Biomedical applications of electrically conductive polymeric systems. e-Polymers 12(1): 722–740

[2] Granström M, Inganäs O (1995) Electrically conductive polymer fibres with mesoscopic diameters: 1. Studies of structure and electrical properties. Polymer 36(15): 2867–2872

[3] Kim DH et al (2007) Effect of immobilized nerve growth factor on conductive polymers: electrical properties and cellular response. Adv Funct Mater 17(1):79–86

[4] Kaur G et al (2015) Electrically conductive polymers and composites for biomedical applications. RSC Adv 5(47):37553–37567

[5] Wang W et al (2014) One-pot fabrication and thermoelectric properties of Ag nanoparticles–polyaniline hybrid nanocomposites. RSC Adv 4(51):26810–26816

[6] Gunatillake PA et al (2003) Designing biostable polyurethane elastomers for biomedical implants. Aust J Chem 56(6):545–557

[7] Gunatillake PA et al (2000) Poly (dimethylsiloxane)/poly (hexamethylene oxide) mixed macrodiol based polyurethane elastomers. I. Synthesis and properties. J Appl Polym Sci 76(14):2026–2040

[8] Gogolewski S (1989) Selected topics in biomedical polyurethanes. A review. Colloid Polym Sci 267(9):757–785

[9] Kathalewar MS et al (2013) Non-isocyanate polyurethanes: from chemistry to applications. RSC Adv 3(13):4110–4129

[10] Hsu S-H, Tang C-M, Tseng H-J (2008) Gold nanoparticles induce surface morphological transformation in polyurethane and affect the cellular response. Biomacromolecules 9(1):241–248

[11] Shukla R et al (2005) Biocompatibility of gold nanoparticles and their endocytotic fate inside the cellular compartment: a microscopic overview. Langmuir 21(23):10644–10654

[12] Daniel M-C, Astruc D (2004) Gold nanoparticles: assembly, supramolecular chemistry, quantum-size-related properties, and applications toward biology, catalysis, and nanotechnology. Chem Rev 104(1):293–346

[13] Matte HR, Subrahmanyam K, Rao C (2009) Novel magnetic properties of graphene: presence of both ferromagnetic and antiferromagnetic features and other aspects. J Phys Chem C 113(23):9982–9985

[14] Sun X et al (2013) Developing polymer composite materials: carbon nanotubes or graphene? Adv Mater 25(37): 5153–5176

[15] Potts JR et al (2011) Graphene-based polymer nanocomposites. Polymer 52(1):5–25

[16] Mittal V, Nuzzo R, Kroto H (2012) Polymer-graphene nanocomposites. Royal Society of Chemistry, London

[17] Stankovich S et al (2006) Graphene-based composite materials. Nature 442(7100):282–286

[18] Kaur G et al (2015) Graphene/polyurethane composites: fabrication and evaluation of electrical conductivity, mechanical properties and cell viability. RSC Adv 5(120):98762–98772

[19] Hsu S-H, Lin Z-C (2004) Biocompatibility and biostability of a series of poly(carbonate)urethanes. Colloids Surf B 36(1):1–12

[20] Shan C et al (2010) Graphene/AuNPs/chitosan nanocomposites film for glucose biosensing. Biosens Bioelectron 25(5):1070–1074

[21] Simmons A et al (2004) Long-term in vivo biostability of poly(dimethylsiloxane)/poly(hexamethylene oxide) mixed macrodiol-based polyurethane elastomers. Biomaterials 25(20):4887–4900

[22] Choi J et al (2013) Facile solvothermal preparation of monodisperse gold nanoparticles and their engineered assembly of ferritin-gold nanoclusters. Langmuir 29(50):15698–15703

[23] Turcheniuk K, Boukherroub R, Szunerits S (2015) Gold–graphene nanocomposites for sensing and biomedical applications. J Mater Chem B 3(21):4301–4324

[24] Mudumba R, Padsalgikar AD, Littler SW (2006) Evaluation of aqueous extracts from Elast-Eon polymers for methylene dianiline (MDA) by high-performance liquid chromatography (HPLC). Aust J Chem 58(12):845–850

[25] Hernandez R et al (2008) In vitro oxidation of high poly-dimethylsiloxane content biomedical polyurethanes: correlation with the microstructure. J Biomed Mater Res Part A 87(2):546–556

[26] Polavarapu L et al (2009) Optical-limiting properties of oleylamine-capped gold nanoparticles for both femtosecond and nanosecond laser pulses. ACS Appl Mater Interfaces 1(10):2298–2303

[27] Ramaraj B (2007) Electrical and mechanical properties of thermoplastic polyurethane and polytetrafluoroethylene powder composites. Polym Plast Technol Eng 46(6):575–578

[28] Compton OC, Nguyen ST (2010) Graphene oxide, highly reduced graphene oxide, and graphene: versatile building blocks for carbon-based materials. Small 6(6):711–723

[29] Ahmad R et al (2015) Nanocomposites of gold nanoparticles@ molecularly imprinted polymers: chemistry, processing, and applications in sensors. Chem Mater 27(16):5464–5478

[30] Zadeh EM et al (2014) Physical and thermal characterization of graphene oxide modified gelatin-based thin films. Polym Compos 35(10):2043–2049

[31] Xu Y et al (2008) Flexible graphene films via the filtration of water-soluble noncovalent functionalized graphene sheets. J Am Chem Soc 130(18):5856–5857

[32] Yousefi N et al (2012) Self-alignment and high electrical conductivity of ultralarge graphene oxide–polyurethane nanocomposites. J Mater Chem 22(25):12709–12717

[33] Rana S, Cho JW, Tan LP (2013) Graphene-crosslinked polyurethane block copolymer nanocomposites with enhanced mechanical, electrical, and shape memory properties. RSC Adv 3(33):13796–13803

[34] Kotzar G et al (2002) Evaluation of MEMS materials of construction for implantable medical devices. Biomaterials 23(13):2737–2750